Synthesis and Properties of a Hole-Conducting, Photopatternable Molecular Glass

Thomas Fuhrmann and Tetsuo Tsutsui*

Department of Applied Science for Electronics and Materials, Graduate School of Engineering Sciences, Kyushu University, Kasuga-Koen 6-1, Kasuga-shi, Fukuoka 816-8580, Japan

Received March 29, 1999. Revised Manuscript Received May 12, 1999

A glass-forming, low molecular weight diaminobiphenyl compound with incorporated azo groups was synthesized. It exhibits a glass transition temperature well above room temperature (101 °C), which is explained in terms of molecular structure. Holographic birefringence gratings as well as surface gratings were produced in thin spin-coated films under intensity and polarization holography conditions. The hole transport property was demonstrated by implementing the material in organic light-emitting diodes. If the special properties of this material are combined, applications such as organic laser diodes with integrated optical feedback gratings seem to be realizable.

Introduction

The interest in organic materials for optical applications has been focused in the past mainly on polymers because of their excellent glass-forming properties which lead to an easy processability as well as optical quality. However, in recent years it has become evident that low molecular weight compounds with an appropriate molecular design may also form stable glasses with glass transition temperatures above 100 °C. These molecular compounds consist of rigid moieties linked by more or less flexible groups such as aliphatic spacer groups[1] or biphenyl bonds[2] or by a spiro connection.[3] At the moment, the development of such molecular glasses is driven in particular by the rapid progress in the field of organic electroluminescence. In this field, molecular glasses are supposed to combine the advantages of molecular materials with those of polymers. First, to avoid any charge carrier traps, high purification is essential for the performance of a device, which is less a problem for low molecular weight materials than it is in the case of polymers. Then, molecular glasses with high glass transition temperature allow the preparation of well-defined, specially functionalized multilayer structures by vacuum vapor deposition while maintaining the morphological stability of polymers, i.e., a reduced tendency of recrystallization and low light scattering effects. The advantages of such multilayer structures are 2-fold. First, by separation of electron transport, hole transport, and emission properties in different layers, the efficiency of an organic light-emitting diode can be significantly improved.[4] In addition, multilayer structures allow the control of optical waveguiding effects which are becoming more and more important with the recent development of edge-emitting organic solid-state lasers.[5−9] While optical pumping in such laser devices has already been demonstrated by many groups, electrical pumping fails because of two reasons: the low rate of photon production because of limited current densities and narrow emission zones and the optical loss in the presence of absorbing electrodes. An improved gain−loss ratio should be obtainable, however, with an efficient waveguide structure, which reduces the loss by separating the waveguide core from the electrodes and increases the gain by introducing a suitable feedback structure. In principle, the formation of optical modes in planar waveguides is suffient for spectral gain narrowing,[5−6] but introducing an optical feedback structure such as a distributed grating decreases the lasing threshold significantly.[7−9] Usually, such a distributed feedback or a distributed Bragg reflector laser is made by etching an appropriate grating into the substrate.

In this work, we present a material which allows another approach for implementing grating structures in multilayer devices. Going back to the original idea of Kogelnik and Shank[10] to write the grating directly into the waveguide core by a photochemical process, we have designed a low molecular weight glass, which can be introduced as a layer in an usual organic light-emitting diode and which can be patterned holographically into a grating structure. We may choose the active emissive layer itself or one of the charge-transporting layers for implementing the grating. In this research, the hole-transporting layer is chosen for the additional

(1) Alig, J.; Braun, D.; Langendorf, R.; Wirth, H. O.; Voigt, M.; Wendorff, J. H. *J. Mater. Chem.* **1998**, *8*, 847.
(2) Kuwabara, Y.; Ogawa, H.; Inoda, H.; Noma, N.; Shirota, Y. *Adv. Mater.* **1996**, *6*, 677.
(3) Salbeck, J.; Yu, N.; Bauer, J.; Weissoertel, F.; Bestgen, H. *Synth. Met.* **1997**, *91*, 209.
(4) Adachi, C.; Tsutsui, T.; Saito, S. *Appl. Phys. Lett.* **1990**, *57*, 531.
(5) Diaz-Garcia, M. A.; Hide, F.; Schwartz, B. J.; McGehee, M. D.; Andersson, M. R.; Heeger, A. J. *Appl. Phys. Lett.* **1997**, *70*, 3191.
(6) Kozlov, V. G.; Bulovic, V.; Burrows, P. E.; Forrest, S. R. *Nature* **1997**, *389*, 362.
(7) Berggren, M.; Dodabalapur, A.; Slusher R. E.; Bao, Z. *Synth. Met.* **1997**, *91*, 65.
(8) Kallinger, C.; Hilmer M.; Haugeneder, A.; Perner, M.; Spirkl, W.; Lemmer, U.; Feldmann, J.; Scherf, U.; Muellen, K.; Gombert, A.; Wittwer, V. *Adv. Mater.* **1998**, *10*, 920.
(9) McGehee, M. D.; Diaz-Garcia, M. A.; Hide, F.; Gupta, R.; Miller, E. K.; Moses, D.; Heeger, A. J. *Appl. Phys. Lett.* **1998**, *72*, 1536.
(10) Kogelnik, H.; Shank, C. V. *Appl. Phys. Lett.* **1971**, *18*, 152.

10.1021/cm9901820 CCC: $18.00
Published on Web 07/10/1999

functionalization. The photochemical principle we chose is based on the photoreorientation of azo dyes by holographic recording which has been so far investigated extensively in the case of liquid crystalline[11] and amorphous[12] side chain polymers. By irradiation with polarized light, azo dyes undergo photoselective isomerization cycles, leading to a reorientation preferably into the plane perpendicular to the polarization direction and therefore to a change in the refractive index ellipsoid. The final orientation is a state in which the molecules cannot be excited again because their transition dipole moment and the polarization direction are perpendicular to each other. By uniform irradiation of an isotropic film with polarized light, uniaxial negative birefringence is induced. Gratings recorded in azo side chain polymers by intensity holography as well as polarization holography[13] using this reorientation principle have been reported by different groups.[11,12,14−18] In many cases, the diffraction effect of the gratings is largely enhanced by additional surface gratings,[16−18] which may arise because of internal shear forces and pressure effects. Applications of the induced gratings in the field of waveguide optics have been demonstrated in a few cases, for instance as input coupling element.[19] In the case of polymers, multifunctional compounds with additional properties such as photorefractive behavior are also under investigation.[20]

In our approach—in order to obtain a low molecular weight system—we combine the azo functionality with a 4,4′-diaminobiphenyl core. Diaminobiphenyl compounds are generally known as glass-forming, highly efficient hole transport molecular materials for organic electroluminescent devices, the most common being *N*,*N*′-bis(3-methylphenyl)-*N*,*N*′-bis(phenylbenzidine) (TPD). From this combination, a hole-transport material is expected, the refractive index of which can be adjusted in well-defined holographic patterns. Because the main effect of the writing mechanism is a molecular reorientation and not a permanent photochemical reaction, no large amount of charge carrier traps are generated as may be the case for a photochemical reaction.

In the following, we describe the synthesis of *N*,*N*′-bis(phenyl)-*N*,*N*′-((4-phenylazo)phenyl)benzidine, which will be called AZOPD hereafter, its glass properties, and experiments for grating patterning and application in light-emitting diodes.

Experimental Section

Materials. 4-Phenylazodiphenylamine was purchased from TCI. 4,4′-Diiodobiphenyl, copper(I) oxide, organic solvents, and other reagents were purchased from WAKO Chemicals. All chemicals are used freshly as supplied without further purification.

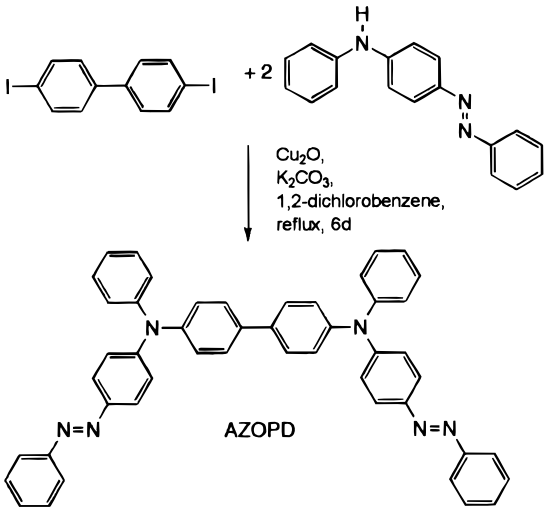

Figure 1. Synthesis scheme of AZOPD.

Synthesis of *N*,*N*′-bis(phenyl)-*N*,*N*′-bis((4-phenylazo)-phenyl)benzidine (AZOPD). The synthesis is performed according to Figure 1 by Ullmann amination. A 0.74 g (1.82 mmol) sample of 4,4′-diiodobiphenyl (M = 406.00), 1.00 g (3.66 mmol) of 4-phenylazodiphenylamine (M = 273.34), 1.0 g (7.2 mmol) of potassium carbonate (M = 138.21), and 0.065 g (0.45 mmol) of copper(I) oxide (M = 143.08) as catalyst were mixed in 75 mL of 1,2-dichlorobenzene, heated to 180 °C, and stirred under reflux for 6 days. After cooling, the reaction mixture was filtrated and washed with water, 10% hydrochloric acid, and again with water. It was dried over magnesium sulfate and filtered, and the solvent was removed by vacuum distillation. The reaction products were separated by column chromatography (WAKO silica gel 300, 200 g, eluent toluene/hexane 3:1). After a small amount of the monosubstituted product was eluted, AZOPD was obtained as the main fraction. It was solved in 10 mL of chloroform and precipitated with ethanol under reflux. The product was filtered, washed with ethanol and dried under vacuum. Yield: 1.00 g (1.44 mmol, 77.9%). Mp: 197 °C. Before application, the product was purified by a second column (WAKO silica gel 300, 300 g, eluent toluene/hexane 2:1) and subsequent recrystallization in 300 mL of 2-methyl-1-propanol.

^{1}H NMR ($CDCl_3$, 600 MHz): 7.87 ppm (“d”, 7.3 Hz, 4H, phenylazo, ortho position), 7.83 ppm (AA′XX′, 9.0 Hz, 4H, *p*-azophenylamine, outer protons), 7.43 ppm (AA′XX′, 8.6 Hz, 4H, biphenyl, inner protons), 7.50 ppm (m, 4H, phenylamine, meta position), 7.43 ppm (m, 2H, phenylazo, para position), 7.34 ppm (“t”, 7.3 Hz, 4H, phenylazo, meta position), 7.22 ppm (m, 8H, biphenyl, outer protons; phenylamine, ortho position), 7.18 ppm (AA′XX′, 9.0 Hz, 4H, *p*-azophenylamine, inner protons), 7.14 ppm (“t”, 7.3 Hz, 2H, phenylamine, para position).

^{13}C NMR: 121.9, 122.5, 124.3, 124.3, 125.4, 125.6, 127.7, 129.0, 129.6, 130.3, 135.9, 146.0, 146.8, 147.4, 150.4, 153.0 ppm.

Anal. Calcd for $C_{48}H_{36}N_6$ (M = 696.88): C, 82.59; H, 5.36; N, 11.90. Found: C, 82.73; H, 5.21; N 12.06.

UV/vis spectrum ($CHCl_3$): λ_{max} = 439 nm (ϵ = 51 000).

Physical Analysis. Differential scanning calorimetry was carried out with a Seiko DSC22 instrument at a heating rate of 10 K/min. UV/vis spectra were taken with a Hitachi 330 spectrophotometer. Film thicknesses were determined with a DEKTAK surface profilometer. AFM surface scans were performed with a Rasterscope3 atomic force microscope.

Sample Preparation. Three different methods for the preparation of thin films were applied. Films of 15 μm thickness for birefringent patterning experiments were prepared by melting in previously prepared cells. The cells had

(11) Eich, M.; Wendorff, J. H.; Reck, B.; Ringsdorf, H. *Makromol. Chem., Rapid Commun.* **1987**, *8*, 59.
(12) Natansohn, A.; Rochon, P.; Gosselin, J.; Xie, S. *Macromolecules* **1992**, *25*, 2268.
(13) Nikolova, L.; Todorov, T. *Opt. Acta* **1984**, *31*, 579.
(14) Anderle, K.; Wendorff, J. H. *Mol. Cryst. Liq. Cryst.* **1994**, *243*, 51.
(15) Nikolova, L.; Todorov, T. *Appl. Opt.* **1996**, *35*, 3835.
(16) Rochon, P.; Batalla, E.; Natansohn, A. *Appl. Phys. Lett.* **1995**, *66*, 136.
(17) Kim, D. Y.; Li, L.; Kumar, J.; Tripathy, S. K. *Appl. Phys. Lett.* **1995**, *66*, 1166.
(18) Ramanujam, P. S.; Holme N. C. R.; Hvilsted, S. *Appl. Phys. Lett.* **1996**, *68*, 1329.
(19) Rochon, P.; Natansohn, A.; Callender, C. L.; Robitaille, L. *Appl. Phys. Lett.* **1997**, *71*, 1008.
(20) Ho, M. S.; Barrett, C.; Paterson, J.; Esteghamatian, M.; Natansohn, A.; Rochon, P. *Macromolecules* **1996**, *29*, 4613.

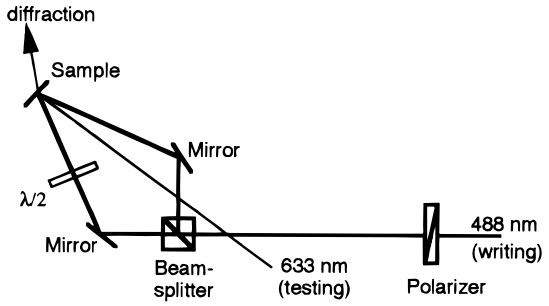

Figure 2. Setup for the holographic experiment.

been constructed by sealing two transparent glass plates, separated by a 15 μm aluminum spacer foil, with a ceramic seal (Aron ceramic). The material was melted into the cell by the means of capillary forces at 210 °C in a vacuum oven, followed by ventilation and rapid cooling to room temperature. Films of 400 nm thickness with a free surface for grating experiments were made by spin-coating of a 5% solution in THF at 3000 rpm (Mikasa 1H−D3 spin-coater) and dried in vacuo at 100 °C for 1 h. Films with thicknesses between 50 and 250 nm were prepared by vacuum vapor evaporation at typical pressures of 4×10^{-4} Pa in an ULVAC EX-400-S evaporation system.

Optical Experiments. All experiments were performed on a vibration-isolated optical table. If not stated otherwise, all optical components and mounts were supplied by Sigma Kouki. As irradiation sources, an argon ion laser (NEC Model GLG 3026) at 488.0 nm was used.

For birefringence patterning experiments, the polarized beam of the argon ion laser is expanded by a spatial filter system (Newport, objective lens 10×, pinhole 25 μm, quartz lens f = 200 mm) for a homogeneous illumination of the sample. A USAF test mask was placed directly before the sample. After the illumination, the copied pattern was observed with a polarizing microscope (Nikon Optiphot 2) and reproduced by a digital camera (Nikon E2I).

The holographic experiments were done with the setup shown in Figure 2. The expanded laser beam is divided by a beam splitter (BK7), the two beams forming an interference pattern at their crossing point. For controlling angle and polarization of the beams, two mirrors (BK7/Al+MgF_2 coating) and a half-wave plate (quartz; wave front distortion all $<\lambda/10$) were used. The sample was placed symmetrically into the crossing point, and the written grating was read out by diffraction of a HeNe laser beam (Toshiba LHG 3217) at 632.8 nm. The intensity of the first diffraction order was monitored by a photodiode with a computer-controlled multimeter (Advantest TR6846).

Results and Discussion

Synthesis, Purification, and Characterization. The synthesis of AZOPD by Ullmann amination[21] is rather straightforward, with satisfactory yields despite the double substitution at the biphenyl core. In this special case, much improvement of the yield was made by using of copper(I) oxide as catalyst instead of copper powder. The good capability of copper(I) oxide as a heterogeneous catalyst in this type of reaction corresponds to similar reports for the synthesis of tertiary aromatic amines without the presence of a base.[22] The presence of air oxygen was found to be advantageous for the catalytic reaction and of no harm to the tertiary amino group which is stabilized by the π-conjugated system of the azo chromophore. On the other hand, decomposition to some extent was observed by maintaining the product at high temperatures in a vacuum for some days. Thus, purification by vacuum train sublimation was not possible. It was confirmed, however, that under the conditions of vacuum vapor deposition, no decomposition product occurs in the condensated film because of the shorter maintaining period at high temperatures and the lesser volatility of the decomposition product. The high molecular weight and the tendency of forming an amorphous glass causes some difficulties in the recrystallization procedure. For almost all solvents, the solubility curves increase only slightly with higher temperatures. With the most suitable solvent, 2-methyl-1-propanol, only about 50% can be recovered in one recrystallization step. Column chromatography, on the other hand, works well for the purification and is the best choice for AZOPD.

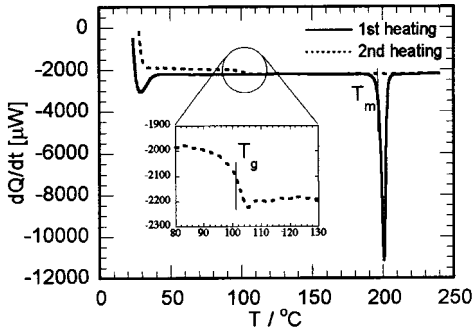

Figure 3. Differential scanning calorimetry curve for AZOPD: solid line, first heating curve with melting point; dashed line, second heating curve with glass−liquid transition behavior.

By differential calorimetry, the melting point was measured to be 197 °C with a melting enthalpy of 48.7 kJ/mol. After the sample was cooled at a moderate cooling rate (2 K/min) and reheated, a glass transition was observed at 101 °C (Figure 3). No melting was detected this time, indicating a complete transition into the vitreous state. The glass transition temperature lies about 40 °C higher than that of TPD which can be understood in terms of molecular structure. Diaminobiphenyls such as TPD and AZOPD can obtain different conformations generated by rotation of the phenyl rings around the connecting bonds. This conformational disorder leads to a prevention of crystallization. The conversion of the conformations is connected with the rotation of rather bulky groups and hence depends on the free volume in the material. Since the chromophore arms of AZOPD have a larger steric demand than phenyl or tolyl groups, the glass transition temperature is increased substantially with respect to TPD.

As optical characterization for thin solid films of AZOPD, we measured the absorption maximum for a solvent-free, vacuum-evaporated film, to be 2.81 eV (441 nm), with a logarithmic absorption coefficient of $\alpha = 1.2 \times 10^7$ m^{-1}. Optical transparent films can prepared by either vacuum evaporation, spin coating or capillary melting into previously prepared cells. The films have low scattering properties, and crystallization becomes apparent only after a few months. Sometimes cracks occur at fast cooling rates of films prepared by capillary melting because of the stiffness of the material. They can be removed, however, by heating for a short time above T_g.

(21) For a review, see: Lindley, J. *Tetrahedron* **1984**, *9*, 1433,
(22) Bacon, R. G. R.; Maitland, D. J. *J. Chem. Soc.* **1970**, 1973.

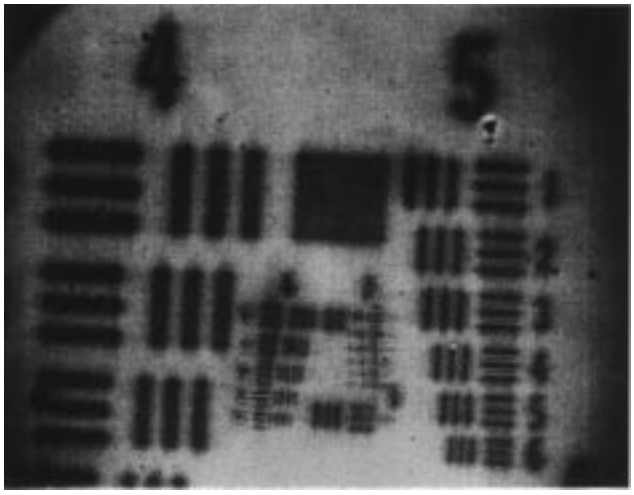

Figure 4. Image of a birefringence pattern (USAF test mask), written through a shadow mask and viewed with a polarizing microscope.

Optical Patterning. The formation of glasses is the necessary condition for the birefringence patterning of azo systems by polarized light. Only in glasses are the different orientational orders through which the orientation process proceeds possible. The condition of formation of a glassy state is fulfilled for the low molecular weight compound AZOPD, but two other crucial questions remain: Is enough free volume provided by the azo isomerization that a reorientation of the bulky chromophores really can take place? Second, is the final orientation stable enough and not be subjected to orientational relaxation processes? The latter occurs for instance in guest−host systems of azo chromophores dispersed in a polymeric matrix, making these systems not suitable for a permanent reorientation process. To answer these questions, we performed mask patterning experiments as well as holographic experiments.

For the mask patterning experiments, cells with a thickness of 15 μm were irradiated through a shadow mask with the polarized light of an argon ion laser operated at 488 nm. The irradiation intensity in these experiments was approximately 2.5 mW/cm^2; the irradiation time was 2 h. Figure 4 shows the copied pattern of the USAF test mask, observed through a polarizing microscope. A resolution of the sixth group, sixth line, which corresponds to 114 lines/mm, was observed by eye. Even after 2 weeks, the birefringence pattern was visible, showing that indeed stable reorientations of molecules can be achieved also in the case of a molecular glass.

By the means of holographic experiments, a much higher resolution avoiding the limiting diffraction effects at the edges of the patterning mask is achieved. In addition, the temporal behavior of birefringence formation and relaxation can be monitored. Since the system is sensitive to both intensity and polarization of the light, intensity gratings (the intensity is modulated, the polarization is constant) as well as polarization gratings (the polarization is modulated, the intensity is constant) may be written into the sample. For writing intensity gratings, we used the interference of two s-polarized laser beams at 488 nm and placed a spin-coated sample of AZOPD with a thickness of 0.4 μm into the interference region (see Figure 2). The angle between the beams

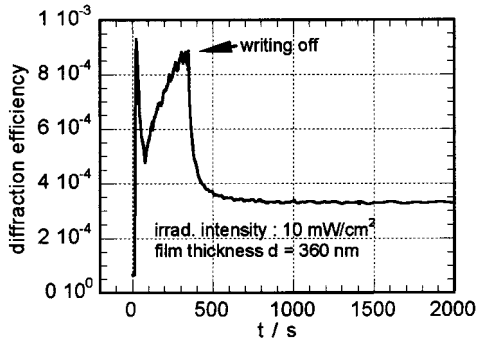

Figure 5. Holographic growth curve for a 360 nm thick film of AZOPD. The experiment was made under intensity holography conditions: both writing beams were s-polarized. After 335 s, the writing light was switched off, and the relaxation was measured.

was adjusted to result in a grating constant of about 1 μm. Figure 5 shows the typical evaluation of the grating diffraction efficiency monitored by diffraction at an reading wavelength of 632.8 nm. At the beginning of the irradiation process there is a peak in the diffraction efficiency resulting from different contributions to the refractive index change. Effects arising from isomerization, thermal heating, and density modulation overlap in this nonequilibrium region. When the system is in thermal equilibrium again, the diffraction efficiency increases steadily. After 5.6 min, the diffraction efficiency reached a saturation value, and the writing light was switched off in order to measure the stability of the grating. A relaxation occurs, but a substantial part (37%) of the signal remains stable. To estimate the maximum modulation of the refractive index, the diffraction theory for thin gratings was applied. In this case, the diffraction pattern is the Fourier transform of the transmission function. If n_1 stands for the modulation of refractive index through the grating

$$n(\delta) = n_0 + n_1 \cos \delta$$

this expression leads to multiple diffraction orders with intensities given in terms of Bessel functions

$$\eta_m = J_m^2(2\pi n_1 d/\lambda(\cos \theta))$$

δ being the phase difference between the two beams, d the film thickness, and λ and θ the reading wavelength and angle, respectively. From the observed first diffraction orders, typical maximum refractive index modulations were calculated to be of the order $n_1 = 1 \times 10^{-2}$. This is the same order of magnitude as in the case of side chain polymers with comparable chromophores. For small diffraction efficiencies, the Bessel functions can be approximated by linear functions, which leads to a quadratic dependence of the diffraction efficiencies on the refractive index modulations. With this approximation, the relaxation curve, was fitted. It was found that a stretched exponential fit

$$n_1(t) = A \exp(-(t/k)^\beta) + B$$

works well for describing the relaxing part as well as the stable part. Typical values for the decay process were $k = 31$ s and $\beta = 0.6$. Since the relaxing part exhibits a broad distribution of relaxation times, it is

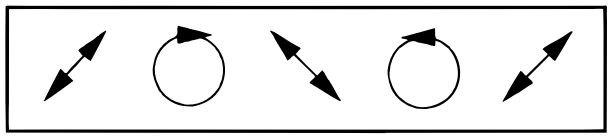

Figure 6. Polarization holography: variation of in-plane polarization caused by the overlap of one s- and one p-polarized writing beam.

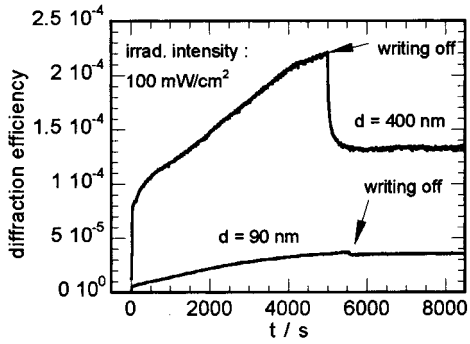

Figure 7. Holographic growth curves for two different samples under polarization holography conditions. The orthogonal polarization of the beams were chosen to be s and p, respectively. After the writing light was switched off, the relaxation was monitored.

likely that not only the thermal relaxation of azo cis isomers but also other processes such as orientational relaxation contribute to this decay. The remaining stable part amounts to 62% in terms of refractive index modulation.

In intensity holography, the theoretical maximum value of refractive index modulation is often not reached because of overwriting effects. These may arise from grating migration due to vibrations in the optical systems or mode oscillations in the laser as well as from differences in the intensities of the two writing beams. The shape of the grating deviates from the sine profile and becomes distorted, until it is finally leveled out, leaving an uniform refractive index distribution. Thus, for the production of gratings with well-defined sine structure and maximum refractive index amplitude, which is desirable for many applications, polarization holography is more suitable. For polarization holography experiments, we switched the polarization of one beam from s to p by inserting a half-wave plate in the appropriate orientation. Thus, the writing beams were orthogonally polarized. In this case, the electric field pattern in the grating exhibits an uniform intensity across the grating but varying polarizations from linear ($\delta = 0$) to circular ($\delta = \pi/2$) to linear ($\delta = \pi$) to circular ($\delta = 3\pi/2$) (for the limit of small writing angles, see Figure 6). It should be pointed out that for large writing angles there is also an electric field component perpendicular to the sample plane, so all spacial directions can be adressed. In each point of the grating, the final orientations of the chromophores are supposed to be perpendicular to the resulting electric field. Even in the case of slow grating migration, the orientational grating will follow the polarization grating in a kind of steady state since the reorientation process is reversible. Thus, the shape of the grating is not distorted, and overwriting effects cannot occur. Figure 7 shows the experimental data for polarization holographic experiments with film of different thicknesses (400 and 90 nm, respectively). In either case, an intensity peak at the beginning like in the case of intensity holography cannot be seen. Instead, the efficiency was rising fast in the first few seconds and then slower until saturation. Under equal irradiation conditions, thinner films reach a lower diffraction efficiency, but the stability of the signal after switching the writing light off is better. The ratio of retained signal after relaxation, however, depends on the irradiation time. To obtain a higher stability of the grating, the irradiation times must be extended. In the case of a 360 nm film, we obtained a stability of 95% in terms of efficiency after 20 000 s irradiation at 100 mW/cm^2.

The question arises whether in the case of low molecular weight materials surface gratings are also formed, as in the case of side chain polymers. The mechanisms of mass transport[21,22] which are the cause for the surface modulations in the latter case are supposed to be different since the chromophores in a low molecular weight material are not connected by a polymeric chain. According to the model of Natansohn et al.,[23] which links the surface grating formation to pressure gradients and the bulk viscosity of the material, surface relief formation should be favorable in low molecular weight materials because of the expected low viscosity of the material under irradiation conditions. On the other hand, a model by Ramanujam et al.,[24] which was made for liquid crystalline systems and focuses on the intermolecular forces, explains the grating formation by a variation of the ordering mean field potential. With respect to this, surface relief formation should not be favorable since these interactions are weak in comparison to liquid crystalline and even amorphous side chain polymers because of the more irregular shape of the molecules. The experimental data are displayed in Figure 8. The surface of the polarization grating written in the 400 nm thick sample of Figure 7 was examined by atomic force microscopy. The AFM surface scan reveals indeed the presence of a surface grating even in the case of the low molecular weight material. The modulation depth is at 9 nm rather small but nevertheless typical for this special type of polarization.[25] Larger modulations are expected for optimized irradiation conditions, i.e., polarization holography with orthogonally circular polarized beams.[25] The grating constant of the sample in Figure 8 was measured to be 1170 nm. This value corresponds to the calculated value of the phase modulation between the two writing beams according to

$$\Lambda = \lambda/(2 \sin \alpha)$$

(Λ, grating constant; λ, writing wavelength; α, incidence angle). Ramanujam et al. predicted for this special type of polarization (writing beams s- and p-polarized, respectively) a grating of twice this spatial frequency, thus leading to a maximum resolution of $\lambda/4$.[24] Unlike in their case of liquid crystalline polymers,[24] this prediction could not be confirmed in the case of the low molecular

(23) Barrett, C. J.; Natansohn, A. L.; Rochon, P. L. *J. Phys. Chem.* **1996**, *100*, 8836.
(24) Pedersen, T. G.; Johansen, P. M.; Holme, N. C. R.; Ramanujam, P. S.; Hvilsted, S. *Phys. Rev. Lett.* **1997**, *80*, 89.
(25) Jiang, X. L.; Kim, D. Y.; Li, L.; Shivshankar, V.; Kumar, J.; Tripathy, S. K. *MRS Symp Proc.* **1996**, *413*, 299.

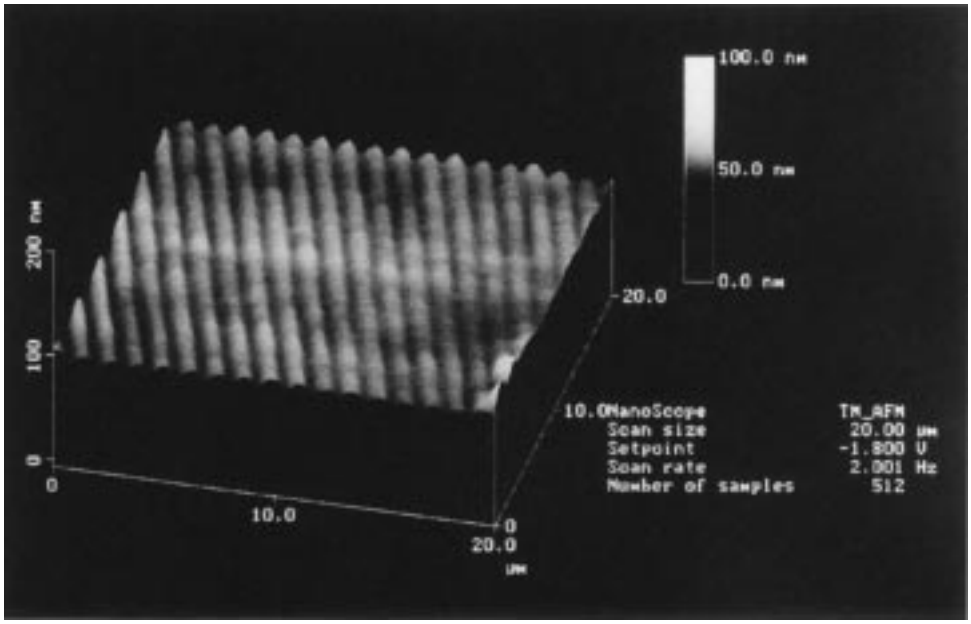

Figure 8. Atomic force microscopy of the surface grating which has formed in the 360 nm thick sample of Figure 7.

weight material AZOPD. At the moment, it is not clear whether this difference is caused by experimental deviations or by the distinct class of materials. However, the model of Ramanujam et al. was made for liquid crystalline systems with strong molecular interactions; thus, it may not be a surprise that it is not applicable in all cases. With this report, we extended the range of materials suitable for surface grating formation toward low molecular mass azo dyes, but still there seem to remain some interesting questions about the differences to side chain polymers.

Application as a Hole-Transport Material. In the last part of this report, we show that not only does AZOPD exhibit the features of photoreorientation due to the azo chromophore but also in addition it has inherited the hole-transporting property of the tertiary diaminobiphenyl core. This is by no means obvious because the electronic structure is substantially altered by introducing the azo group. The ability to exhibit hole injection and transport depends on the HOMO energy level and the delocalization of charge in the radical cation in order to have an optimum overlap with neighboring molecules. Unlike the situation for simpler diaminobiphenyl derivatives, the electronic structure of AZOPD can be described with n- and π-type molecular orbitals in the upper energy levels. The n-type orbitals are localized at the lone electron pairs of the azo nitrogen atoms; the π-type orbitals are delocalized over the molecule. In a radical cation, localizing a positive charge in n-type orbitals would act as a trap and prevent hopping transport. The absorption spectrum of AZOPD, however, shows a low-energy $\pi\pi^*$ excitation, indicating that a state with π-delocalized charge may be the most favorable state for the cation. Thus, the molecule is expected to be hole transporting as the other diaminobiphenyls. To demonstrate this, we fabricated electroluminescent devices incorporating AZOPD as a hole-transporting layer. They consist of a 2 mm wide and 200 nm thick ITO (indium−tin−oxide) electrode on a glass substrate, followed by a 50 nm layer of AZOPD and 75 nm aluminum tris(hydroxychinolin) ($Al(q)_3$), doped with the dye 4-(dicyanomethylene)-2-methyl-6-(*p*-dimethylaminostyryl)-4*H*-pyran (DCM). By coevaporation of $Al(q)_3$ and DCM, the concentration of the dopant was controlled to be 2.5%. The doping was necessary in order to shift the emission wavelength of the device away from the absorption band of AZOPD. On top of the device, a 2 mm wide, 110 nm thick electrode of Mg:Ag (10:1) was deposited. Indeed, emission was observed under electric driving conditions. The luminance vs voltage characteristic of this double layer device is shown in Figure 9. For a fresh sample, a maximum luminance of 50 cd/m^2 at 17 V was achieved. After keeping the sample for half a year in a vacuum desiccator, the measurement was made again. Electroluminescence was still achieved, with a shift of the threshold voltage of about 7 V. This shift is mainly contributed to the oxidation of the MgAg electrode rather than crystallization of the hole transport material. By microscopic investigation of the sample, no crystallization was detected. The current−luminance characteristics and the spectrum of the device are shown in Figure 10. As characteristic of the emission system, they did not change with storing time. Since azo dyes are normally not fluorescent, DCM—which is excited via Förster transfer from $Al(q)_3$—is the only emitter in this

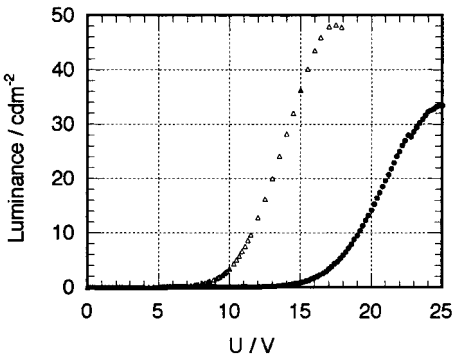

Figure 9. Voltage−luminance characteristic of an electroluminescent device consisting of substrate/ITO/AZOPD/$Al(q)_3$: DCM/MgAg: empty marks, fresh device; filled marks, device after storage for half a year under vacuum.

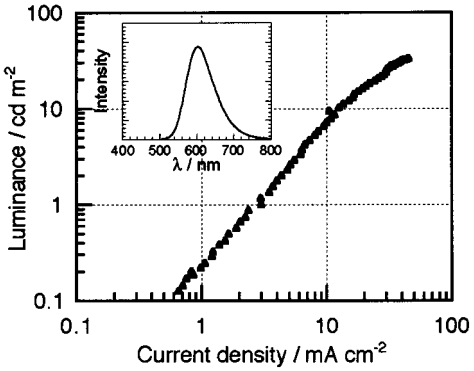

Figure 10. Current density−luminance characteristic of the device in Figure 9. Inset: Electroluminescence spectrum. The emission band is the characteristic band of the dye DCM.

device. These experiment demonstrate the general ability of AZOPD as a hole-transporting material in electroluminescent devices. More detailed investigations such as the comparison with other hole transporting materials with respect to energy levels and charge mobilities are in progress.

Conclusion and Outlook

It was shown that AZOPD exhibits all the properties needed for applications in electrically driven light emission diodes with an integrated optical feedback grating: It is a glass with a high glass transition temperature, it can be patterned into grating structures, and it shows hole-transporting properties. Multilayer devices incorporating AZOPD should be possible, in which defined feedback gratings can be written directly. As light emission layer in such structures, the $Al(q)_3$/DCM system may be very useful here, since it has been already proven to be suitable for photopumped lasing devices.[6,7] We believe that this may one of the promising pathways toward the development of an organic distributed feedback laser diode.

Acknowledgment. This contribution was partly supported by CREST/JST and by the Japanese Ministry of Education (Monbusho) with a postgraduate scholarship.

CM9901820